

Effect of ITO surface condition on the characteristics of organic static induction transistors based on pentacene films

Y. Watanabe¹, H. Iechi^{1, 2} and K. Kudo^{1, 3}

¹OPTOELECTRONIC INDUSTRY AND TECHNOLOGY DEVELOPMENT ASSOCIATION (OITDA),
Advanced Organic Device Project, Chiba Laboratory, 1-33 Yayoicho, Inage-ku, Chiba,
Fax: 81-43-290-2709, e-mail: watanabe@restaff.chiba-u.jp,

²Advanced Technology R&D Center, Research and Development Group, Ricoh Co. Ltd,
16-1 Shinei, Tsuzuki, Yokohama,
Fax: 81- 45-590-1911, e-mail: hiroyuki.iechi@nts.ricoh.co.jp

³Department of Electronics and Mechanical Engineering, Faculty of Engineering, Chiba University,
1-33 Yayoicho, Inage-ku, Chiba.
Fax: 81- 43-290-3039, e-mail: kudo@faculty.chiba-u.jp

Organic static induction transistors (OSITs) based on pentacene thin-film have been fabricated on a indium-tin-oxide (ITO) formed on the glass substrates. It is well known that the work function of ITO is controlled by the method used to clean its surface. We have fabricated the OSITs based on pentacene thin film with the high work function ITO of 5.3 eV and the low work function ITO of 4.2 eV. The influence of the work function of ITO on the static characteristics was investigated by means of current-voltage measurement and ultraviolet photoemission spectroscopy (UPS) measurement. These results provided an important clue that the higher on/off ratio of 50 for the organic SIT was achieved by the formation of the hole injection barrier, which works as tunneling layer on a source electrode. The barrier works effectively as controlling a tunnel current from a source electrode by applying the gate voltage.

Key words: OSITs, pentacene, ITO, work function, UPS, hole injection barrier,

1. INTRODUCTION

In the beginning of the research, organic thin-film transistors (OTFTs) were fabricated to investigate the basic electrical parameters such as carrier mobilities in the organic semiconductor films.[1] At the present day, OTFTs have been very attractive device to the application for photovoltaic cell and organic light-emitting devices (LEDs).[2,3] OTFTs have attracted much attention for the application in the field of portable or ubiquitous devices[4] such as flexible display[5] and radio-frequency identification tags[6] due to their lightweight and mechanical flexibility. In addition, OTFTs have possibility to fabricate low-cost electronic applications on plastic so that OTFTs could be fabricated on flexible substrate at room temperature.

However, OTFTs have several disadvantages including low current density, high operational voltage, and low speed of operation due to their high resistivity and low carrier mobility.[7-10] To improve the device performance, organic static induction transistors (OSITs), which utilize organic semiconductors, have been employed.[11-15] Recently, we have succeeded to fabricate the OSITs on the flexible plastic substrate.[16]

The SITs are promising device because it enables high-speed and high-power operation.[17] The excellent characteristics of the SIT are known to be due to the vertical structure, with a very short channel length corresponds to the thickness of an organic semiconductor film between the source and drain electrodes. The slit-type Al gate electrodes were inserted into the organic semiconductor layer.

The conventional OSITs mentioned above were fabricated on a source electrode formed on a substrate without the investigation of the influence of the work

function of source electrodes on the device characteristics. In this study, OSITs based on pentacene thin films was fabricated on the indium-tin-oxide (ITO) as the source electrodes on the glass substrates. The ITO is widely used as a transparent and conductive electrode in organic light-emitting diodes (OLEDs).[18] Pentacene is one of the most promising materials due to its high field-effect mobility.[19-20] To achieve the high on/off ratio and high current values in the OSITs, we have studied the influence of the work function of the ITO on the static characteristics of the OSITs. It is well known to that the work function of ITO was controlled by the method used to clean its surface.[21]

2. EXPERIMENTAL PROCEDURE

Figure 1 shows a schematic diagram of a fabricated pentacene SITs. The effective area of the source and drain electrodes of the OSIT is approximately 2.25 mm². The devices are fabricated by conventional vacuum evaporation with the substrate temperature maintained at

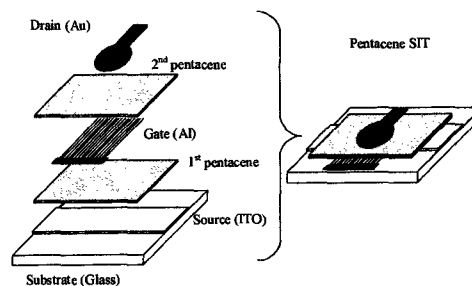


Fig. 1. Schematic diagram of pentacene SITs on the ITO formed on glass substrates.

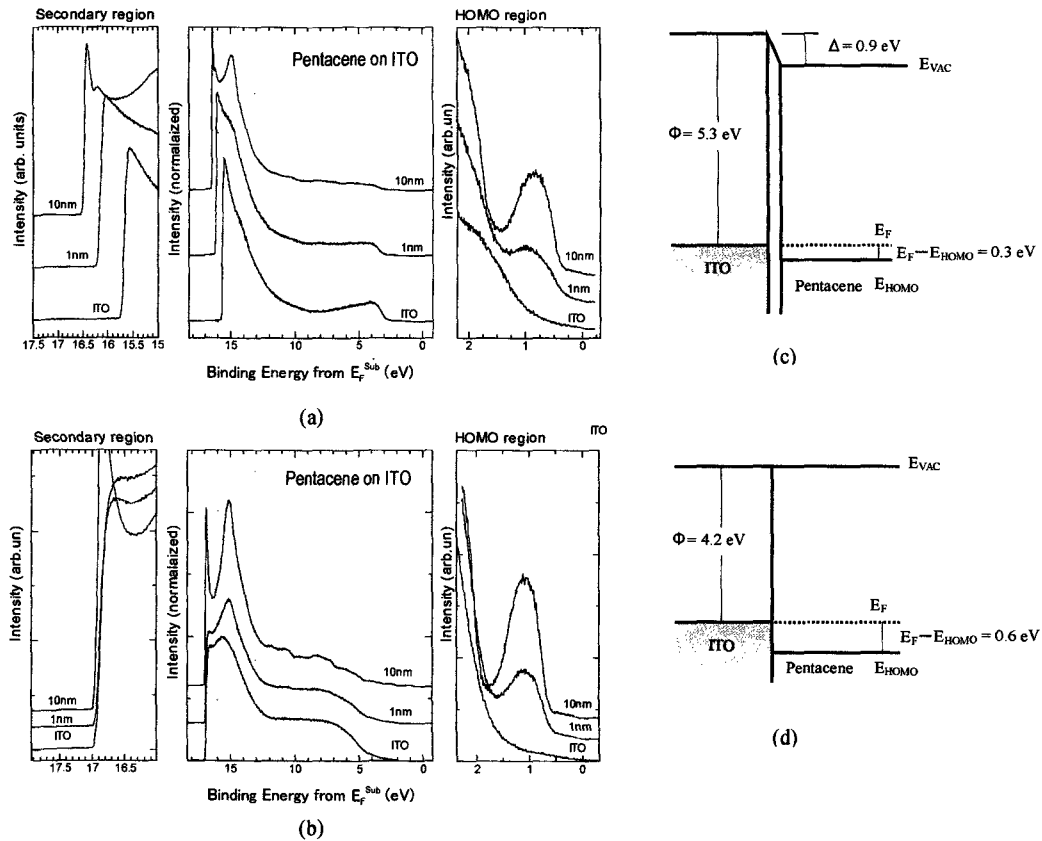


Fig. 2. UPS He II (21.22 eV) spectra of pentacene/low work function ITO (a) and pentacene/high work function ITO (b). Energy band diagram of pentacene/low work function ITO (a) and pentacene/high work function ITO (b).

room temperature during the vacuum deposition. The fabrication process is as follows. First, a 100 nm pentacene thin film is deposited on the ITO formed on the glass substrate. Second, a slit-type Al gate electrode with a thickness of 30 nm is formed on the pentacene film by using a shadow evaporation method. Third, the Al gate electrode is covered with a second 100 nm pentacene film. Finally, the drain Au with a thickness of 30 nm is fabricated on the pentacene film. The pentacene films are evaporated under a vacuum of 2×10^{-4} Pa and the source temperature of the pentacene and the evaporation rate are 200°C and 0.1 nm/s, respectively. The fabrication process is described in Ref. [16] in detail.

The ultraviolet photoemission spectroscopy (UPS) measurements were performed to evaluate the energetic position of Fermi and highest occupied molecular orbital (HOMO) levels for metallic and organic surfaces, respectively. From these results, the hole injection barriers at the interface between the electrode and the organic layer were estimated. We monitored the electrical properties using a semiconductor parameter analyzer (4156C, Agilent). All electrical measurements were performed in air at room temperature. The measurements were carried out in the dark in order to obtain the OSIT characteristics without the photovoltaic effect of the Schottky barrier contact.

3. RESULTS AND DISCUSSION

3.1 Surface treatment and work function of ITO

In this section, we report that the surface cleaning method on the work function of ITO. The work function of ITO is extremely sensitive to the method used to clean its surface. [21] An example of the UPS spectrum of the ITO is shown in Fig. 2 for different methods to clean its surface. Spectra (a) and (b) were measured with He I ($h\nu = 21.2$ eV) photons. In the UPS spectrum, the work function is the difference between the kinetic energy measured at the detector for electrons at the cut-off plus the photon energy, and the energy of the electrons originating from the Fermi level of the sample as shown in the secondary region. In addition, the HOMO level is the binding energy from the Fermi level (E_F^{Sub}) as shown in the HOMO region. In this study, the high work function of ITO substrates was obtained by subjecting to ultrasonic agitation in water, acetone and isopropanol and then exposing to isopropanol vapor. In UV-ozone treatment, after solvent cleaning the substrate was exposed to UV-ozone treatment for 5 min. In this case, the work function of ITO seems to be approximately 5.3 eV as shown in the secondary region of Fig. 2 (a). [22] The HOMO of pentacene on ITO is assumed to be 4.8 eV as shown in the HOMO region of Fig. 2 (a). In this case, a change in the position of the pentacene vacuum level as a function of the thickness (1 nm–10 nm) was observed. On the other hand, the low work function of ITO was obtained by the same process mentioned above without UV-ozone treatment. In this case, the work function of ITO seems to be approximately 4.2 eV as shown in the secondary region of Fig. 2 (b). [21] The HOMO of pentacene on ITO is assumed to be 4.8 eV as shown in

HOMO region of Fig.2 (a). [23] In this case, no change in the position of the pentacene vacuum level as a function of the thickness (1 nm-10 nm) was observed. Figure 2 (c), (d) shows the energy band diagram at the interfaces of the pentacene/ITO. The hole injection barrier is formed at the interfaces by the difference between the work function of the ITO and the HOMO band of the pentacene. From these results, it was found that the hole injection barrier at the interface of pentacene/low work function ITO is higher than that of pentacene/high work function ITO.

3.2 Static characteristics for pentacene SITs

The operating mechanism of the OSITs was explained as follows. The injected hole carriers from the source flow toward the drain region through the saddle point of the potential barrier at the gate. The current flow of the OSIT is controlled by the potential barrier height depending on the Al gate applied voltage. In other words, the current from source to drain is restricted by spreading the depletion layer around the Al Schottky gate electrode under positive gate voltage.

Before measuring the static characteristics of the OSIT, the differences in I - V characteristics between the gate and source electrodes, and the gate and drain electrodes are measured to confirm formation of a Schottky barrier near the Al gate electrode. The resulting I - V curves exhibit rectification property, with a forward bias corresponding to a negative voltage applied to the gate Al electrode. The experimental results are in good agreement with the results reported by other authors; that is, the pentacene films show p-type semiconducting properties, forming a Schottky barrier contact with the Al gate electrode. In addition, the avalanche breakdown point was not seen until an applied gate voltage of +5 V. In addition, the current-voltage (I - V) characteristics between the source and drain electrodes were measured under the floating gate condition. In the case of the pentacene SITs on the high work function ITO, a symmetrical I - V curve was exhibited at the drain applied voltage from -3 V to +3 V. This indicates that the hole injection from ITO electrode was similar to that of Au. Based on these results, the pentacene/ITO contact have a high efficiency at hole injection due to a small difference between the work function of ITO and the HOMO of pentacene as depicted in Fig. 2 (c). And then, in the case of the pentacene SITs on the low work function ITO, an asymmetrical I - V curve was exhibited at the drain applied voltage from -3 V to +3 V. This indicates that the hole injection barrier was higher than that of the pentacene SIT on the high work function ITO as depicted in Fig. 2 (d).

We also measured static characteristics such as the source-drain current (I_{DS}) as a function of the source-drain voltage (V_{DS}). To operate the OSITs, it is important that the voltage range applied to each electrode does not adversely affect the Schottky barrier around the gate electrode. In the experiment, V_{DS} was changed continuously from 0 V to -3 V while the gate voltage (V_G) was changed from approximately -0.8 V to +2.5 V. Figure 3(a) and 3(b) show the static characteristics for the pentacene SIT on the high work function ITO and the low work function ITO, respectively. In both samples, I_{DS} at a constant V_{DS} decreases with increasing V_G . This phenomenon demonstrates that the majority carriers of

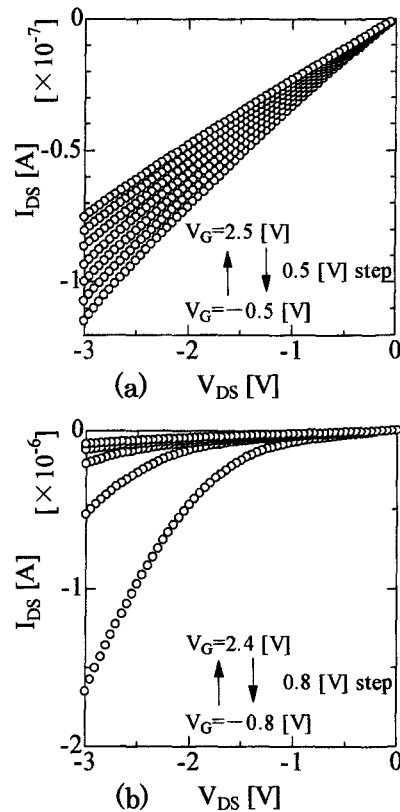


Fig.3. Static characteristics of the pentacene SIT on the high work function ITO (a) and the low work function ITO (b).

holes in the pentacene flow from the source to the drain and are controlled by gate voltage V_G applied to the Al Schottky gate electrode. These results indicate that the on/off ratio for the pentacene SITs on the low work function ITO was higher than that on the high work function ITO. On the other hand, the current values were almost the same with changing the ITO work function.

These results demonstrate that at a constant drain voltage higher than the threshold voltage for the pentacene SITs on the low work function ITO, the source region is filled with hole and the hole injection barrier as a tunneling barrier thickness becomes thinner and the hole injection barrier height becomes lower as the negative gate voltage is applied. The tunneling hole flows from source to drain, which decreases with increasing the gate applied voltage and increases with decreasing gate applied voltage. This phenomenon can be explained by the presence of the hole injection barrier as a tunneling barrier.

Here, Fowler-Nordheim tunneling theory [24] was referred to confirm the presence of the tunneling current in I_{DS} . If the gradient is negative in Fowler-Nordheim plot (FN plot), the tunneling current was contained in I_{DS} . Figure 4(a) and 4(b) show $\ln(-I_{DS}/V_{DS}^2)$ vs $-1/V_{DS}$ characteristic known as FN plot of the static characteristics for the pentacene SIT on the high work function ITO and the low work function ITO, respectively. They were characterized to conform the dependence of the gate voltage V_G on the tunneling current in drain-source current I_{DS} . In case of the plot for the SIT on the high work function ITO, the negative gradient was not seen due to the absence of the tunneling current. On

the other hand, in the plot for the SIT on the low work function ITO, the deviation from the negative gradient at higher V_{DS} is likely to be due to the tunneling current.

These results demonstrate that the formation of the carrier injection barrier works as a tunneling barrier at the pentacene / ITO interface is effective to fabricate the high

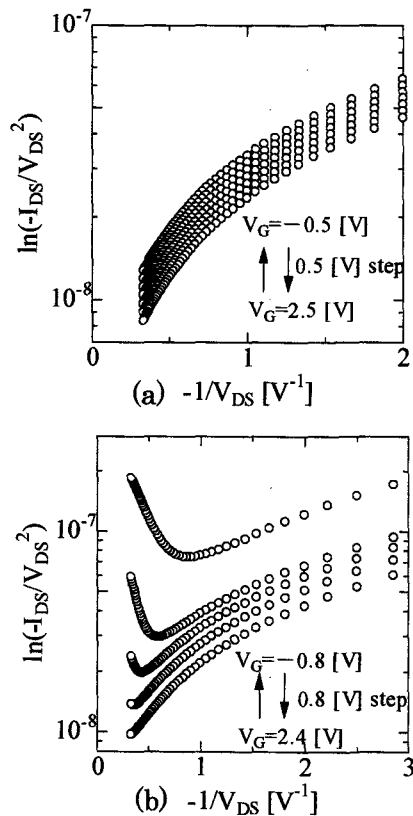


Fig.4. Fowler-Nordheim plot of the static characteristics for the pentacene SIT on the high work function ITO (a) and the low work function ITO (b).

performance organic SITs.

4. CONCLUSIONS

We can find the clear correlation between the static characteristics of a pentacene SIT and the interface condition of pentacene/ITO as a source electrode by changing the ITO work function. As a result, it is necessary to form the hole injection barrier works as tunneling layer on a ITO as a source electrode to achieve the high on/off ratio for the organic SIT. The barrier works effectively as controlling a tunnel current from a source electrode by applying the gate voltage. From the UPS measurement in this study, the energy band diagram at the interface of pentacene/ITO was clear to understand the mechanism for operating of the OSITs. However, the influence of the work function of ITO on the energy band condition at the interface of the pentacene/ITO requires further investigation by means of atomic force microscope to observe the morphology at the surface, X-ray diffraction measurement to investigate the crystallinity of the pentacene film and so on. This research is currently progressing towards the fabrication of the high performance OSITs.

Acknowledgements

A part of this work belongs to "Advanced Organic Device Project" which OITDA contracted with New Energy and Industrial The author are grateful to Dr. N. Ueno and H. Fukagawa, R. Fukaya, T. Kataoka, and S. Hosoumi for many helpful discussion.

References

- [1] K. Kudo, M. Yamashina and T. Morizumi, *Jpn. J. Appl. Phys.* **23**, 130 (1984).
- [2] T. Morizumi and K. Kudo, *Appl. Phys. Lett.* **38**, 85-86 (1981).
- [3] C. W. Tang and S. A. VanSlyke, *Appl. Phys. Lett.* **51**, 913-915 (1987)
- [4] Stephen R. Forrest, *Nature* **428**, 911-918 (2004).
- [5] Anna B. Chwang, a) Mark A. Rothman, Sokhanno Y. Mao, Richard H. Hewitt, Michael S. Weaver, Jeff A. Silvermail, Kamala Rajan, Michael Hack, and Julie J. Brown, *Appl. Phys. Lett.* **83**, 413-415 (2003).
- [6] P. F. Baude, D. A. Ender, M. A. Haase, T. W. Kelly, D. V. Muyres and S. D. Theiss, *Appl. Phys. Lett.* **82**, 3964-3966 (2003).
- [7] A. Tsumura, H. Koezuka, T. Ando, *Appl. Phys. Lett.* **49**, 1210-1212 (1986).
- [8] G. Guiland, M. A. Sadoun, M. Maitrot, J. Simon, M. Bouvet, *Chem. Phys. Lett.* **167**, 503-506 (1990).
- [9] Y. Y. Lin, D. J. Gundlach, S. F. Nelson, T. N. Jackson, *IEEE Trans. Electron. Devices* **44**, 1325-1331 (1997).
- [10] A. Dodabalapur, Z. Bao, A. Makhjia, J. G. Laquindanum, V. R. Raju, Y. Feng, H. E. Katz, J. Roger, *Appl. Phys. Lett.* **73**, 142-144 (1998).
- [11] K. Kudo, D. X. Wang, M. Iizuka, S. Kuniyoshi and K. Tanaka, *Thin Solid Films* **331**, 51-54 (1998).
- [12] D. X. Wang, Y. Tanaka, M. Iizuka, S. Kuniyoshi, K. Kudo and K. Tanaka, *Jpn. J. Appl. Phys* **38**, 256-259 (1999).
- [13] K. Kudo, D. X. Wang, M. Iizuka, S. Kuniyoshi and K. Tanaka, *Synth. Metals* **111-112**, 11-14 (2000).
- [14] K. Kudo, M. Iizuka, S. Kuniyoshi and K. Tanaka, *Thin Solid Films* **393**, 362-367 (2001).
- [15] S. Zorba and Y. Gao, *Appl. Phys. Lett.* **86**, 193508 (2005).
- [16] Y. Watanabe and K. Kudo, *Appl. Phys. Lett.* **87**, 223505 (2005).
- [17] J. Nishizawa, T. Terasaki and J. Shibata, *IEEE Trans. Electron Devices* **22**, 185-197 (1975).
- [18] C. W. Tang and S. A. VanSlyke, *Appl. Phys. Lett.* **51**, 913-915 (1987).
- [19] S. F. Nelson, Y.-Y. Lin, J. Gundlach and T. N. Jackson, *Appl. Phys. Lett.* **72**, 1854-1856 (1998).
- [20] O. D. Jurchescu, J. Baas and Thomas T. M. Palastra, *Appl. Phys. Lett.* **84**, 3061-3063 (2004).
- [21] K. Sugiyama, H. Ishii, Y. Ouchi and K. Seki, *Appl. Phys.* **87**, 10140-10146(2000).
- [22] S. M. Tadayyon, H. M. Grandin, K. Griffiths, P. R. Norton, H. Aziz and Z. D. Popovic, *Organic Electronics* **5**, 157-166 (2004).
- [23] M. Obarowska, R. Singnerski and J. Godlewski, *J. Luminescence* **112**, 337-340 (2005).
- [24] I. D. Parker, *J. Appl. Phys.* **75**, 1656-1666 (1994).

(Received December 10, 2005; Accepted March 2, 2006)